International Journal of Vehicle Safety

ISSN online: 1479-3113 - ISSN print: 1479-3105
https://www.inderscience.com/ijvs

Evaluation of human seated posture exposure to low-frequency vibrations using biodynamic model

Mangesh Phate, Shraddha Toney, Vikas Phate

DOI: 10.1504/IJVS.2022.10054755

Article History:

Received:	16 February 2021
Accepted:	07 March 2022
Published online:	17 March 2023

Evaluation of human seated posture exposure to low-frequency vibrations using biodynamic model

Mangesh Phate*

Department of Mechanical Engineering,
AISSMS College of Engineering,
Pune, Maharashtra, India
Email: mangeshphate03@gmail.com
*Corresponding author

Shraddha Toney

Department of Computer Engineering AISSMS,
Institute of Information and Technology,
Pune, Maharashtra, India
Email: toneyshraddha@gmail.com

Vikas Phate

Department of Electronics & Telecommunication Engineering,
Government Polytechnic Amravati,
Pune, Maharashtra, India
Email: vikas.phate13@gmail.com

Abstract: In this paper, the biodynamic responses exposed to human seated posture were investigated by developing a biodynamic model based on anthropometric data for various Indian male subjects. Four degrees of freedom model for the human seating posture was constructed to extract the different biodynamic responses at several low-frequency vibrations. The male subjects were categorised by age and body weight. A total of nine different categories were identified for the examination. The impact of body mass, age, stiffness, and damping coefficient of the body segments was analysed using MATLAB-based code. The biodynamic responses of seated posture have been measured in terms of seat-to-head transmissibility (STHT), driving point impedance (DPMI), and apparent mass (AM). The present work will help to predict the biodynamic responses of the seated human body under various vertical excitations. The results of the current work show that the proposed approach was very much effective and reliable for designing a seated posture ergonomically.

Keywords: seating posture; four DOF; human vibration; DPMI; STHT; AM; anthropometric; biodynamic.

Reference to this paper should be made as follows: Phate, M., Toney, S. and Phate, V. (2022) 'Evaluation of human seated posture exposure to low-frequency vibrations using biodynamic model', *Int. J. Vehicle Safety*, Vol. 12, Nos. 3/4, pp.253–280.

1 Introduction

The human body is a sophisticated dynamic system whose mechanical properties vary from person to person and time. Biodynamic model for the human body as mass elements is connected by springs and dampers. This type of model is very simple to analyse and easy to validate with experiments. Many people are daily exposed to noise and vibration generated environments while travelling and working places. Generally, many heavy-duty vehicles like tractors and trucks expose drivers to a high level of vibration in their occupational lives, which causes vibration-induced injuries or disorders. The responses such as AM and DPMI express 'to-the-body' vibration while STHT expresses 'through-the-body' vibration impact. The current study proposed a 4-DOF analytic biomechanical model of the human body in a sitting posture without backrest in vertical vibration direction to investigate different masses' biodynamic responses and stiffness.

Liu et al. (2017) examined how forces affect the body-seat interface. Vertical and fore-and-aft forces were measured middle thighs and front thighs of 14 subjects sitting on a rigid flat seat in three postures with different thigh contact while exposed to random vertical vibration at three magnitudes. Liang and Chiang (2006) concluded that the lumped-parameter models have limited to dimensional analysis. Therefore, this study's human body considered sitting erect without backrest support irrespective of hands' position, while feet are supported and vibrate. These mathematical models include linear and nonlinear systems with varying degrees of complexity. Sastry et al. (2018) investigated the impact of vehicular vibrations on the human body. Magnetorheological (MR) dampers-based semi-active suspension system was developed and analysed for a 7 DOF human body model (Fairley and Griffin, 1989). They measured five postures for one subject (slouched, normal, slightly erect, erect and very erect) and four postures for eight subjects (normal, erect, with backrest, tense). They found that the mean apparent mass resonant frequency increased with the erect posture, and the magnitude of this frequency slightly decreased for the eight subjects. However, results for the one subject showed otherwise. Both the magnitude and frequency of the single subject's apparent mass increased with the more erect posture.

Gupta (2007) considered a 15 Degree of Freedom human model. The background available to this work was the approach of Nigam and Malik. They proposed that an undamped spring-mass vibratory model of the human body can be framed through the anthropomorphic model using anthropomorphic data and some elastic properties of bones and tissues. The problem was then to introduce damping in the basic spring-mass model. Marzbanrad et al. (2010) investigated the impact of vibration using MR dampers. The optimisation of the responses is done by using a genetic algorithm. The optimised model was integrated with the nonlinear model. Feng (2019) investigated automobile seat design based on ergonomics principles for providing human comfort. The parameters such as dimensions of the seat, backrest, inclination, posture physiology and the distribution of the body mass along the seat were examined during the analysis. Rao et al. (2018) reviewed the bus seats subjected to vibration during the shuttle and school bus services' extended seating posture. The effect of seat inclination, speed, and seat position was investigated using statistical software.

Abdeen and Abbas (2010) explained that ANN models presented in their study are very useful in analysing the effect of the human body's mass and stiffness on the biodynamic response behaviours under whole-body vibration. They interpreted that the

ANN-based approach was very effectively used in the analytic solution of the model. Based on the results of implementing the ANN technique in their study. From the analysis and validation, Neil (2005) explained that exposure to whole-body vibration is a risk factor for developing low back pain. To create a fuller understanding of the seated person's response to beat, they conducted experiments in the laboratory investigating the seated person's biomechanics. Some of their methods are based on the driving force and acceleration at the seat. They are reported in their literature as apparent mass, driving point mechanical impedance, or absorbed power. Phate et al. (2019); Phate and Sahu (22020); Phate and Gaikwad (2018) and Phate et al. (2022) investigated the impact of vibration on human seated posture using various soft computing techniques such as response surface method and artificial neural network. Six degrees of freedom models were developed for the analysis. The experimental result shows that the approach was useful for the study. Govindan and Harsha (2018) investigated various human bodies' dynamic characteristics using a 3D finite element model. The model was tested for the different low-frequency vibrations. Nigam and Malik (1987) proposed anthropomorphic models to develop a generalised approach for human body vibratory modelling resorting to an experimental program. They created a linear undamped lumped parameter model based on the anthropomorphic model of Bartz and Gionottiin, in which the segments were identified as ellipsoids.

The model's novel feature was in the determination of masses and stiffness of the various elements of the model. An investigation also studied the influence of a backrest and variation in a seated posture conducted by Wang et al. (2008) to measure the apparent mass response characteristics of twenty-four human subjects seated in representative automotive postures hands-in-lap and hands-on-steering-wheel. The measurements were carried out under white noise vertical excitations of 0.25, 0.5 and 1.0 ms^{-2} r.m.s. Acceleration magnitudes in the 0.5–40 Hz frequency range. Bai et al. (2017) proposed and demonstrated a methodology for systematically identifying the best configuration or structure of a 4-degree-of-freedom (4DOF) human vibration model its parameter identification. To help understand seated human occupants' biodynamic responses and design anti-vibration devices and test dummies, it is of great importance to establish effectual biodynamic models. 4DOF lumped-parameter biodynamic models have drawn attention for a long time.

2 Method

The biodynamic responses calculated by using some anthropometric dimensions of the human body. The various sizes consider in the present work are as tabulated in Table 1. The flow of analysis is as shown in Figure 1. In the initial phase, the various male subjects of different categories shown in Figure 2 selected for the investigation. After that, the anthropometric data tabulated in Table 2 measured for each subject, then the mass-damper model called biodynamic model with 4-DOF model suggested by Nigam and Malik (1987) (see Figure 3) was developed and the values for the mass, stiffness and damping coefficient calculated using biodynamic standards based on the body dimensions as tabulated in Tables 3 and 7. A soft code developed using MATLAB, and the responses were measure for each male subject. The answers are analysed, and the impact of variation in mass, stiffness and the damping coefficient was investigated for the analysis. In the next section of the paper, the detailed procedure will be presented:

Table 1 Anthropometric dimensions and notations

Symbol	*Dimensional data*	*Symbol*	*Dimensional data*	*Symbol*	*Dimensional data*
W	Weight of object	L7	Head breadth	L24	Abdomen height
L1	Standing height	L8	Head to chin height	L25	Abdomen breadth
L2	Shoulder height	L9	Neck circumference	L26	Abdomen depth
L3	Armpit height	L10	Shoulder breadth	L27	Thigh circumference
L4	Waist height	L11	Chest depth	L28	Shoulder to elbow length
L5	Seated height	L12	Chest breadth	L29	Knee height seated
L6	Head length				

Table 2 Anthropometric measurements of all male subjects

Symbol	*Parameter*	*Measurements of subjects*								
		M1	*M2*	*M3*	*M4*	*M5*	*M6*	*M7*	*M8*	*M9*
M	Mass (Kg)	49.9	64.6	82	53	66	83	43.85	70.3	83.6
A	Age (Years)	18	22	22	26	30	35	71	47	54
BMI	Body mass index	17.06	24.92	27.48	17.91	24.21	25.05	17.08	22.88	34.75
L1	Standing height	171	161	172.7	172	165.1	182	160.2	175.2	155.1
L2	Shoulder height	140.4	131	141.4	141.6	135	150.2	136.5	145	130.5
L3	Armpit height	132.3	124	133.6	133.8	127.6	140	129.7	136	121.3
L4	Waist height	98.6	90.5	98.9	98.8	93.1	106	97.3	100.2	90.3
L5	Seated height	131.5	127.7	131.9	132	128.2	135	121.8	132	124
L6	Head length	20.2	21.3	22	20.3	21.6	21.3	19.6	21.7	23
L7	Head breadth	18.5	21	20.2	18.91	20.3	20.7	16.9	26.5	20.2
L8	Head to chin height	15.7	14.3	16.7	15.9	16.5	17.3	15.3	17	17
L9	Neck circumference	33.6	35.5	36.6	34	36.3	35	36	36.3	42
L10	Shoulder breadth	41.6	45.8	46	42.8	46.5	47	41	47.2	46
L11	Chest depth	14.2	20	22	16	31.1	30.1	18.2	32.3	28.5
L12	Chest breadth	32.2	33.1	33.7	32.6	33.26	32	31.56	34.1	33.26
L24	Abdomen height	23.4	23.2	29.6	29.7	23.3	24	19.7	23.8	33.2
L25	Abdomen breadth	25.1	31.4	33	28.9	28.9	29	24	29	35
L26	Abdomen depth	17.6	24.2	30	19.8	23	23.1	18.8	24	32.8
L27	Thigh circumference	44.5	50	60	47	56	54.2	36.7	56	62
L28	Shoulder to elbow	34.8	35	35	34.9	36	31.7	35.2	33	31.5
L29	Knee height seated	51.2	50	51	51.3	50.2	53	49	51.3	50

Figure 1 Flow of research work

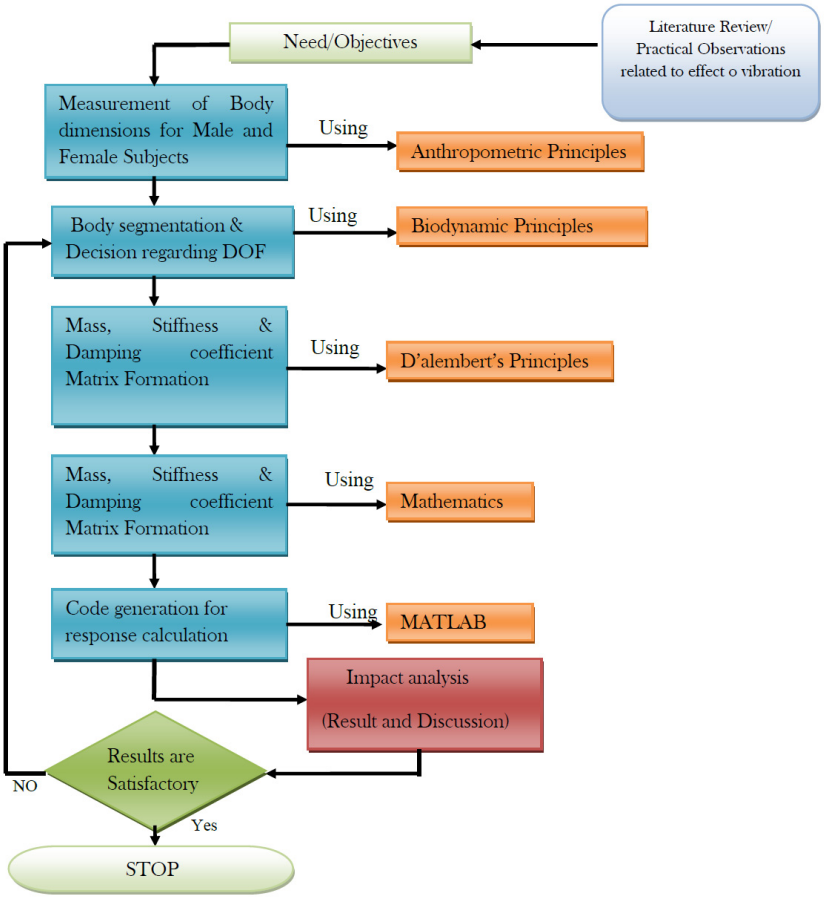

Figure 2 Selection of male objects for the investigation

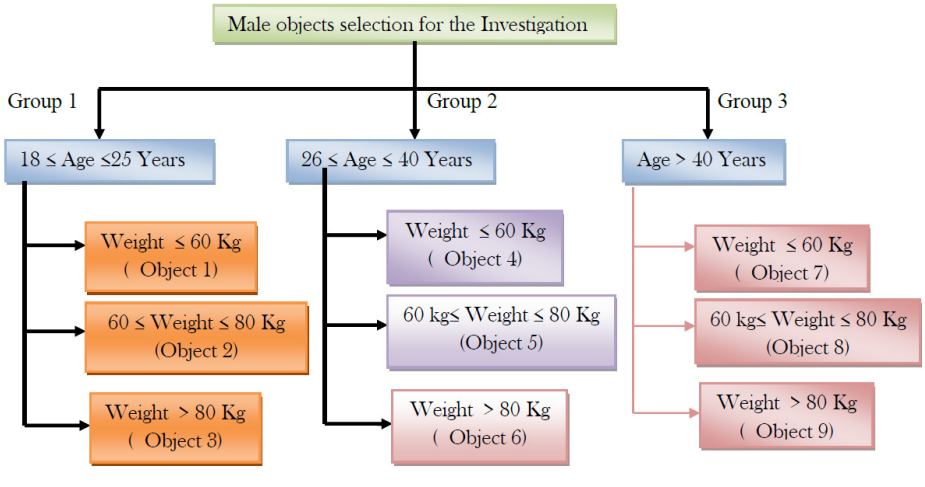

3 Analytical model formulation

3.1 Body segmentation

In this section, anthropometric based model formulation of a human seated posture exposed to the vertical vibrations is discussed systematically. The seated human body is divided into four segments as head, upper torso, thorax, diaphragm, abdomen and thigh, as shown in Figure 3. After the object's segmentation in the human body in four DOF model (Wang et al., 2008), the next step is to form the various vibrational equations. The fundamental motion equation for the developed 4-DOF model is given by equation (1).

$$\begin{aligned}
M_1\ddot{X}_1 &= -C_1*\left(\dot{X}_1-\dot{X}_2\right)-K_1*\left(X_1-X_2\right)\\
M_2\ddot{X}_2 &= C_1*\left(\dot{X}_1-\dot{X}_2\right)+K_1*\left(X_1-X_2\right)-C_2*\left(\dot{X}_2-\dot{X}_3\right)-K_2*\left(X_2-X_3\right)\\
M_3\ddot{X}_3 &= C_2*\left(\dot{X}_2-\dot{X}_3\right)+K_2*\left(X_2-X_3\right)-C_3*\left(\dot{X}_3-\dot{X}_4\right)-K_3*\left(X_3-X_4\right)\\
M_4\ddot{X}_4 &= C_3*\left(\dot{X}_3-\dot{X}_4\right)+K_3*\left(X_3-X_4\right)-C_4*\left(\dot{X}_4-\dot{X}_{se}\right)-K_4*\left(X_4-X_{se}\right)
\end{aligned} \tag{1}$$

Figure 3 Developed 4-DOF human body vibratory model (Wang et al., 2008).

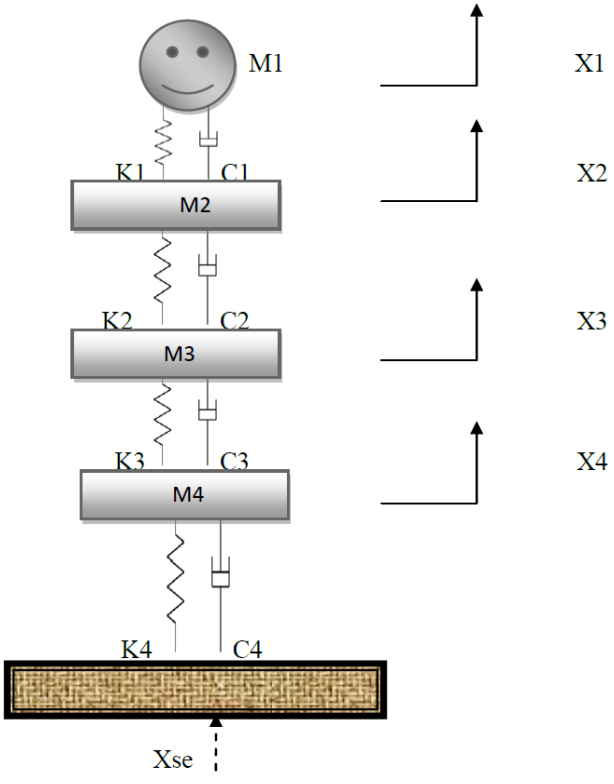

The above equations of motion can be reframed and as given by equation (2)

$$[M]*\{\ddot{X}\}+[C]*\{\dot{X}\}+[K]*\{x\}=\{f\} \tag{2}$$

where [*M*], [*K*] and [*C*] are the matrices for mass, stiffness and damping coefficient respectively. While the $\{f\}$ is the force vector due to external excitation. The *M*, *K*, *C* and excitation force matrix are calculated by the following equations (2a) to (2d):

$$[M]=\begin{bmatrix} M1 & 0 & 0 & 0 \\ 0 & M2 & 0 & 0 \\ 0 & 0 & M3 & 0 \\ 0 & 0 & 0 & M4 \end{bmatrix} \tag{2a}$$

$$[C]=\begin{bmatrix} C1 & -C2 & 0 & 0 \\ -C1 & C1+C2 & -C2 & 0 \\ 0 & -C2 & C2+C3 & -C3 \\ 0 & 0 & -C3 & C3+C4 \end{bmatrix} \tag{2b}$$

$$[K]=\begin{bmatrix} K1 & -K2 & 0 & 0 \\ -K1 & K1+K2 & -K2 & 0 \\ 0 & -K2 & K2+K3 & -K3 \\ 0 & 0 & -K3 & K3+K4 \end{bmatrix} \tag{2c}$$

$$\{f\}=\begin{Bmatrix} 0 \\ 0 \\ 0 \\ C_4\dot{X}_{se}+K_4X_{se} \end{Bmatrix} \tag{2d}$$

The Fourier transformation of equation (2) is reframed as equation (3)

$$\left\{-\omega^2[M]+j\omega[C]+[K]\right\}^{-1}.Z(j\omega)=Fz(j\omega) \tag{3}$$

Where the complex phasor $j=\left(\sqrt{-1}\right)$ and ω is the angular frequency. The solution of the above equation is presented by equations (4a) to (4b)

$$Z(j\omega)=Z1(j\omega),Z2(j\omega),Z3\left(j[\omega),Z4(j\omega)\right]^T \tag{4a}$$

$$[0,0,0,Fz(j\omega)=\left(K_4+j\omega C_4\right)Z_0(\omega)=\begin{bmatrix} 0 & 0 \\ 0 & 0 \\ 0 & 0 \\ K_4 & C_4 \end{bmatrix}\begin{bmatrix} 1 \\ j\omega \end{bmatrix}Z_0(j\omega) \tag{4b}$$

Solving equations (3) and (4), $Z(j\omega)$ can be reframed as equation (5).

$$Z(j\omega)=A^{-1}B\begin{bmatrix} 1 \\ j\omega \end{bmatrix}Z_0(j\omega) \tag{5}$$

With $A = -\omega^2[M] + j\omega[C] + [K]$ (6a)

$$B = \begin{Bmatrix} 0 & 0 \\ 0 & 0 \\ 0 & 0 \\ K_4 & C_4 \end{Bmatrix} \quad (6b)$$

Solving equations (5) and (6), the dynamic response Z various unknown parameters are calculated.

3.2 Calculations of Mass (M), stiffness (K) and damping coefficient(C)

- *Mass calculation for 4 DOF human biodynamic model*: These measurements used for the analysis of mass, stiffness and damping co-efficient of human body segments. Nigam and Malik (1987) proposed the use of an anthropomorphic-based human seated four-degree model. The various components identified as ellipsoids (see Figure 4).

Figure 4 (a) An elliptical segment (b) Truncated ellipsoidal

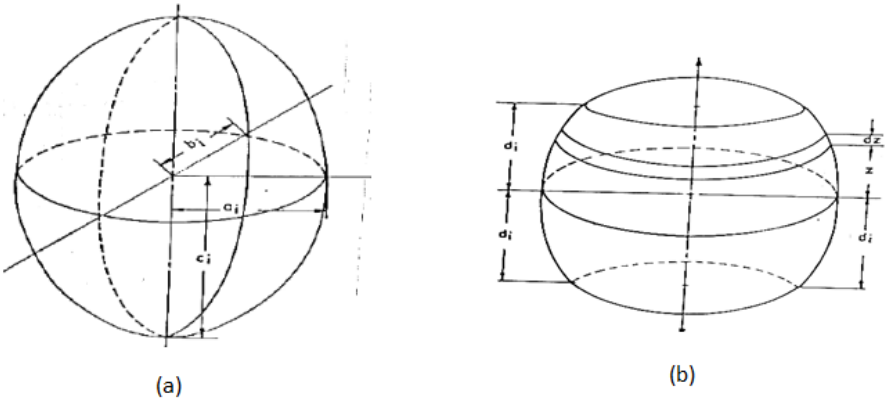

where a_i, b_i, c_i are semi-axes of i-th ellipsoidal segment in x-, y-, z-axes, respectively and they are calculated according to following formulae described in Table 3.

Table 3 Statistical dimensions of ellipsoids representing human body segments

Body segment	*Mass element (kg)*	*Formulae*		
		a_i	b_i	c_i
Head+ Neck	M_1	(L7/2)+(L8/2π)	(L7/2)+(L8/2π)	(L6/2)+((L1-L2-L6)/2)
Upper Torso	M_2	(L13/2)	(L14/2)	(L12/2)
Lower Torso	M_4	(L25/2)	(L26/2)	(L24/2)
Thigh	M_5	(L27/2π)	(L27/2π)	((L2-L28-L29)/2)

M_i is the mass of that particular segment and it may be expressed as equation (7):

$$M_i = \frac{M * V_i}{\sum_{j=1}^{n} V_j} \quad \text{kg} \tag{7}$$

where

V_i = Volume of *i*-th segment = $\pi * a_i * b * c_i$

a_i, b, c_i are the semi axes of the ellipsoid.

n = Total number of segments

M = Total body mass

- *Spring stiffness of a human body segment*:

For evaluating the stiffness of the segment, the axial tension of a truncated ellipsoid is considered. Because of the assumptions regarding the mechanical properties and neglecting the strains due to the self-weight compared to those caused by the forces a body may have to withstand, the expression for axial stiffness S_i of the ellipsoid may be derived as equation (8).

$$S_i = \frac{\pi * E * a_i * b_i}{C_i * l_i} \quad \text{kN/m} \tag{8}$$

where

$$E = \left(E_b * E_t\right)^{\frac{1}{2}} \tag{9}$$

E = Elastic Modulus of Human Body (13.06 MN/m^2)

E_b = Elastic Modulus of Bone (22.6 GN/m^2)

E_t = Elastic Modulus of Tissue (7.5 kN/m^2)

d_i is the half length of the truncated ellipsoid.

$$Ii = \log\left(\frac{2 - tr'}{tr'}\right) \tag{10}$$

where

$tr' = 1 - \frac{d_i}{c_i}$ may be referred to as the truncation factor.

Same ellipsoidal segment have been used by Nigam and Malik (1987) in their vibratory model and truncation of 5% at both the ends i.e. $di = 0.95 * c_i$. In this work also same truncation factor is assumed, therefore segmental stiffness can be expressed as -

$$Si = \frac{0.857524 \times E\, a_i b_i}{c_i} \quad \text{kN/m}$$

Substituting value of $E = 13.06$ MN/m^2,

$$= \frac{11164.277 a_i b_i}{c_i} \quad \text{kN/m} \tag{11}$$

By using 'equations (9) to (11)' Segmental stiffness is calculated and stiffness of spring element (K_i) is calculated is shown in 'Table 4'.

Table 4 Stiffness calculation of segmental body element

Body segment	*Stiffness of spring element (kN/m)*	*Formulae*
Head and Neck	K_1	S_1
Upper Torso	K_2	$S_2S_3/(S_2+S_3)$
Lower Torso	K_3	$S_3S_4/(S_3+S_4)$
Thighs	K_4	S_4

- *Damping coefficient of human body segments :* Damping ratio is defines as the ratio of damping coefficient over critical damping, where critical damping depends upon the square root of stiffness and mass of the system and it is required to bring the system back into equilibrium in minimum time. The damping ratio of *i*-th segment is given by 'equation (12)'

$$\xi_i = \frac{\beta_i}{2 * \sqrt{S_i * M_i}} \tag{12}$$

hence,

$$\beta_i = \xi_i * 2 * \sqrt{S_i M_i} \ (\text{kN-s/m}) \tag{13}$$

above equation is used to calculate damping constant of the *i*-th body segment.

where

ξ_i = Damping ratio of the *i*-th segment

β_i = Damping constant of the *i*-th segment (N-s/m)

S_i = Stiffness of the segment (kN/m)

M_i = Mass of the segment (kg).

Certain range of damping ratio of the segments has been given in Table 5.

Table 5 Range of damping ratio values for different body segment

Sr. No.	*Body segment*	*Damping constant* (ξ_i)
1	Head and Neck	0.009445
2	Upper Torso	0.3212
3	Lower Torso	0.675
4	Thighs	0.5

After calculating all body segmental damping constants, we can calculate damping constants for the human vibratory model as per formulae given below in Table 6.

Table 6 Damping constants of the vibratory model

Body segment	*Damping constant for body segments (kN-s/m)*	*Formulae*
Head and Neck	C_1	$2\beta_1\beta_2/(\beta_1+\beta_2)$
Upper Torso	C_2	$2\beta_2\beta_3/(\beta_2+\beta_3)$
Lower Torso	C_3	$2\beta_3\beta_4/(\beta_3+\beta_4)$
Thighs	C_4	$2\beta_3$

- *Human biodynamic responses*:
- *Seat to head transmissibility (STHT)*: Transmissibility is defined as the ratio of the acceleration at a point on the body $a_{body}(f)$ at frequency '*f*' to the acceleration at the seat point $a_{seat}(f)$ at same frequency. The STHT is calculated using following equation (14a):

$$STHT\ or\ T(f) = \frac{a_{head}(f)}{a_{seat}(f)} \tag{14a}$$

- *Driving point mechanical impedance (DPMI)*: The point which is in contact with the vibrating surface and has a major impact of it is known as the driving point of a system. The measurements of the driving force and acceleration is only made at this point, usually at the seat or floor.

DPMI is defined as the complex ratio of the driving force $'F(f)'$ and velocity $'v(f)'$ at the frequency $'(f)'$. Hence, The DPMI is calculated using following equation (14b),

$$DPMI\ or\ z(f) = \frac{F(f)}{v(f)}\ \text{SI unit of DPMI is Ns/m} \tag{14b}$$

Usually the velocity is not measured directly but can be calculated from acceleration which can be determined either in the time domain by integrating the acceleration – time history or in the frequency domain.

$$a(f) = 2\pi f * v(f)$$

$$z(f) = 2\pi f * \frac{F(f)}{a(f)}$$

- *Apparent mass (AM)*: Newton's second law states that 'The rate of change of momentum of a body is proportional to the force acting on it and it is in the direction of force' hence $-F = m * a$, where F is force, m is mass and a is acceleration. For rigid mass systems this equation holds at all frequencies, however for a non-rigid system such as the human body; the force required to accelerate the supporting surface is a complex function of frequency. This complex function of frequency is termed as Apparent Mass (AM) or *M(F)*. The value of semi-ellipsoids for the various male subjects is as shown in Table 7. The AM is calculated using following equation (14c):

$$AM \text{ or } M(f) = \frac{F(f)}{a(f)}, \text{ SI unit of AM is kg} \tag{14c}$$

AM is usually calculated in frequency domain. The *AM* of a rigid body is not the function of frequency but is equal to its static mass. For non-rigid body such as human body, this means that the *AM* is not a function of their dynamic character but also a function of their supported weight.

Table 7 Values of semi-axes of ellipsoids

Segment No.	*Segment designation*	*Magnitude of semi axes of ellipsoids in (cm) computed from Table 3.*		
		a_i	b_i	c_i
Values of semi-axes of ellipsoids for M1				
1	Head + Neck	11.7487	11.7487	15.3
2	Upper Torso	16.1	7.1	15.75
3	Lower Torso	12.55	8.8	11.7
4	Thigh	7.0823	7.0823	28.85
Values of semi-axes of ellipsoids for M2				
1	Head + Neck	16.0385	16.03859	15
2	Upper Torso	16.55	10	17.4
3	Lower Torso	15.7	12.1	11.6
4	Thigh	7.957747	7.957747	23.1
Values of semi-axes of ellipsoids for M3				
1	Head + Neck	15.67042	15.67042	15.66
2	Upper Torso	16.85	11	17.5
3	Lower Torso	16.5	15	14.8
4	Thigh	9.549297	9.549297	27.7
Values of semi-axes of ellipsoids for M4				
1	Head + Neck	15.02542	15.02542	15.2
2	Upper Torso	16.3	8	17.5
3	Lower Torso	14.45	9.9	14.85
4	Thigh	7.480282	7.480282	27.65

Table 7 Values of semi-axes of ellipsoids (continued)

Segment No.	*Segment designation*	*Magnitude of semi axes of ellipsoids in (cm) computed from Table 3.*		
		a_i	b_i	c_i
Values of semi-axes of ellipsoids for M5				
1	Head + Neck	15.70451	15.70451	15.05
2	Upper Torso	16.63	15.55	17.45
3	Lower Torso	14.45	11.5	11.65
4	Thigh	8.912677	8.912677	24.95
Values of semi-axes of ellipsoids for M6				
1	Head + Neck	16.07958	16.07958	15.9
2	Upper Torso	16	15.05	18
3	Lower Torso	14.5	11.55	12
4	Thigh	8.626198	8.626198	30.6
Values of semi-axes of ellipsoids for M7				
1	Head + Neck	13.49521	13.49521	11.85
2	Upper Torso	15.78	9.1	15.85
3	Lower Torso	12	9.4	9.85
4	Thigh	5.840986	5.840986	27.9
Values of semi-axes of ellipsoids for M8				
1	Head + Neck	18.85225	18.85225	15.13
2	Upper Torso	17.05	16.15	17.6
3	Lower Torso	14.5	12	11.9
4	Thigh	8.912677	8.912677	29.25
Values of semi-axes of ellipsoids for M9				
1	Head + Neck	15.35211	15.35211	12.3
2	Upper Torso	16.63	14.25	16.5
3	Lower Torso	17.5	16.4	16.6
4	Thigh	9.867606	9.87606	23.75

- *Calculating values of body segmental volume:* Calculating segmental volume for each body segments of all the objects i.e. v_1, v_2, v_3, v_4 and V as per the formula described in the previous section is tabulated in Table 8.

Let, v_1 = Segmental volume of Head + Neck, v_2 = Segmental volume of Upper Torso, v_3 = Segmental volume of Lower Torso, v_4 = Segmental volume of Thighs and V = Total segmental volume of all 4 body segments.

Table 8 Volumes for body segments

Subject No.	*Magnitude of segmental volume in (cm^3)*				
	v_1	v_2	v_3	v_4	V
M1	6634.731	5656.068	4059.403	4546.278	20896.48
M2	12121.98	9046.844	6922.977	4595.599	32687.4
M3	12081.01	10190.15	11507.65	7935.465	41714.27
M4	10780.7	7169.114	6673.895	4860.5	29484.21
M5	11660.98	14176.46	6081.931	6226.396	38145.77
M6	12915.06	13616.92	6313.659	7153.361	39998.99
M7	6779.968	7150.354	3490.561	2990.381	20411.26
M8	16893.33	15225.08	6504.982	7299.482	45922.87
M9	9107.335	12284.03	14967.18	7265.025	43623.57

- *Calculation for Mass of body segments:* Calculating mass of each body segment for all objects is tabulated in Table 9.

where m_1 = Segmental mass of Head + Neck, m_2 = Segmental mass of Upper Torso, m_3 = Segmental mass of Lower Torso and m_4 = Segmental mass of Thighs.

Table 9 Final mass calculations

Subject No.	*Segmental masses of the subjects*			
	m_1	m_2	m_3	m_4
M1	15.84349	13.50648	9.693699	10.85634
M2	23.95663	17.87925	13.68186	9.082267
M3	23.74828	20.03133	22.62122	15.59917
M4	19.37909	12.887	11.99681	8.737102
M5	20.17588	24.52819	10.52299	10.77294
M6	26.79941	28.25582	13.10117	14.8436
M7	14.56557	15.36127	7.498854	6.424306
M8	25.86078	23.30696	9.958005	11.17425
M9	17.45325	23.54106	28.68303	13.92266

- *Calculation for stiffness calculations of objects:* Calculating segmental stiffness of each body segment i.e. S_1, S_2, S_3 and S_4 for all objects is tabulated in Table 10 where, S_1 = Segmental stiffness of Head + Neck, S_2 = Segmental stiffness of Upper Torso, S_3 = Segmental stiffness of Lower Torso and S_4 = Segmental stiffness of Thighs.

Table 10 Segmental stiffness calculations

Subject No.	*Magnitude of segmental stiffness in (kN/m)*			
	S_1	S_2	S_3	S_4
M1	100721.3	81027.84	105383.1	19410.87
M2	191457.3	106189	182834.3	30605.46
M3	175065.4	118245.6	186699.9	36753.07
M4	165821.3	83189.81	107549.2	22592.87
M5	182954.4	165446.6	159246.7	35544.82
M6	181544.4	149353.2	155811.4	27148.64
M7	171582	101146.2	127850.8	13652.08
M8	262251.7	174668.6	163242.4	30319.43
M9	213925.1	160344.4	193020.9	45771.02

- *Stiffness of the spring element :* Calculating stiffness of the spring element of each body segment i.e. K_1, K_2, K_3 and K_4 for all objects is tabulated in Table 11.

where,

K_1 = stiffness spring element of Head + Neck,

K_2 = stiffness spring element of Upper Torso,

K_3 = stiffness spring element of Lower Torso,

K_4 = stiffness spring element of Thighs.

Table 11 Final stiffness of the spring element

Subject no.	*Magnitude of spring stiffness in (kN/m)*			
	K_1	K_2	K_3	K_4
M1	100721.3	45807.22	16391.64	19410.87
M2	191457.3	67174.47	26216.89	30605.46
M3	175065.4	72394.73	30708	36753.07
M4	165821.3	46907.02	18670.71	22592.87
M5	182954.4	81143.72	29058.74	35544.82
M6	181544.4	76257	23120.17	27148.64
M7	171582	56470.72	12334.94	13652.08
M8	262251.7	84381.15	25570.21	30319.43
M9	213925.1	87585.91	36997.75	45771.02

- *Damping coefficient calculations of objects:* Calculating damping constant of each body segment i.e. β_1, β_2, β_3 and β_4 for all objects; is tabulated in Table 12.

where β_1 = Damping constant of Head + Neck, β_2 = Damping constant of Upper Torso, β_3 = Damping constant of Lower Torso, β_4 = Damping constant of Thighs.

Table 12 Damping constants of body segments

Subject no.	Magnitude of damping constant in (kN-s/m)			
	β_1	β_2	β_3	β_4
M1	23.86261	672.0378	1364.47	459.0545
M2	40.45579	885.156	2135.183	527.2257
M3	38.51662	988.6736	2774.366	757.1773
M4	33.86248	665.1454	1533.452	444.2929
M5	36.29273	1294.098	1747.586	618.8072
M6	41.6664	1319.674	1928.806	634.8097
M7	29.86286	800.7446	1321.852	296.1505
M8	49.19397	1296.152	1721.22	582.0626
M9	36.50069	1248.089	3176.497	798.2822

- *Damping coefficient of the segment:* Calculating damping coefficient of each body segment i.e. C_1, C_2, C_3 and C_4 for all objects; by using all necessary formulae and data from 'Tables 7 and 13'.

where,

$C1$ = Damping coefficient of Head + Neck,

$C2$ = Damping coefficient of Upper Torso,

$C3$ = Damping coefficient of Lower Torso,

$C4$ = Damping coefficient of Thighs.

Table 13 Final damping coefficient of body segment

Subject no.	Magnitude of damping coefficient in (N-s/m)			
	C_1	C_1	C_1	C_1
M1	46.08871	900.5372	686.984	2728.941
M2	77.37518	1251.495	845.6428	4270.366
M3	74.14473	1457.833	1189.671	5548.733
M4	64.44412	927.8357	688.9684	3066.904
M5	70.60534	1487.036	913.9805	3495.171
M6	80.78225	1567.13	955.2327	3857.612
M7	57.57841	997.3313	483.8894	2643.705
M8	94.79029	1478.745	869.9391	3442.44
M9	70.9271	1792.055	1275.915	6352.994

3 Results and discussion

In the present work, the human body was divided into four parts (4DOF) as per the Boileau and Rakheja model. The parameters such as mass, stiffness and damping coefficients are calculated on the basis of anthropometric and biodynamic correlations –

the selection of male subjects based on age and weight (see Figure 2). In the following section, the impact of variation in the mass, stiffness and damping coefficient is discussed.

3.1 Analysis of impact of mass variation on the vibratory responses

Nine different male subjects of body weight (49.9, 64.6, 82, 53, 66, 83, 43.85, 70.3, 83.6 kg) were used to investigate the impact of mass variation on the biodynamic responses STHT, DPMI and AM, respectively. The effect of the interpretation of mass as per the identified male subject is shown in Figures 5(a), 5(b) and 5(c), respectively. From these figures, it observed that with the increase in the body mass, the response STHT, DPMI and AM increased. The impact vibrations are severe in the higher age male with the higher weight than the young male subject. From the above figures, it can be seen that the human biodynamic response is directly propositional to the body weight and age.

Figure 5 (a) Impact of mass on STHT response on male objects (b) Impact of mass on DPMI response on male objects (c) Impact of mass on AM response on male objects (see online version for colours)

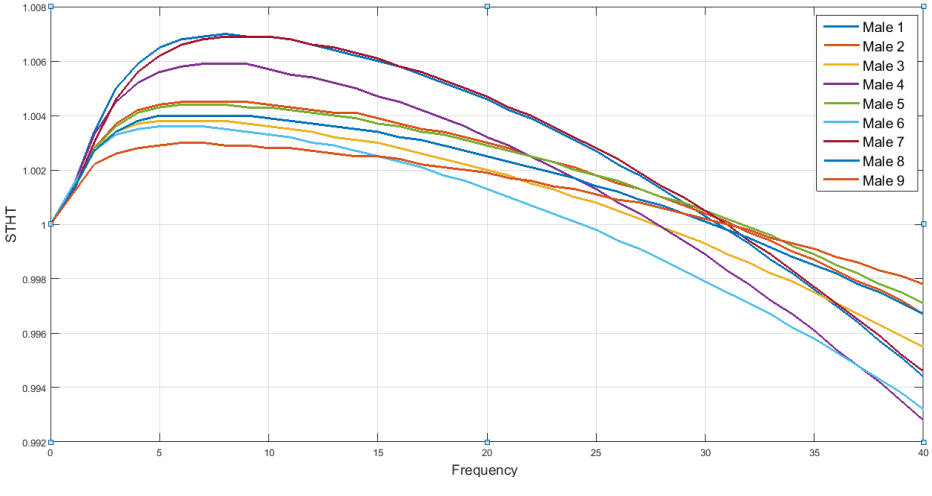

(a)

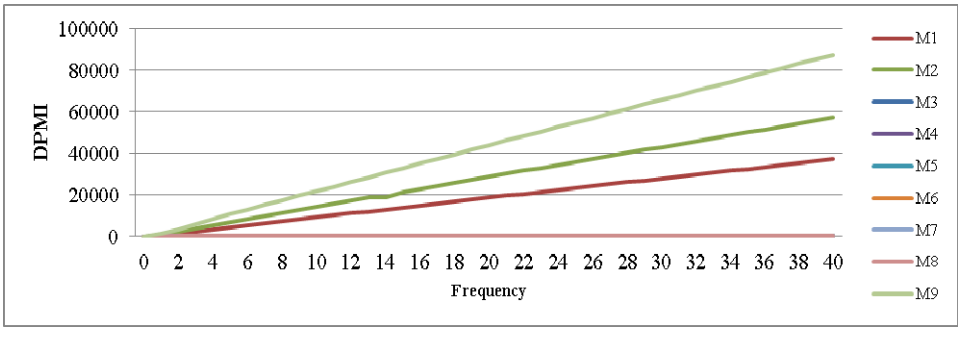

(b)

Figure 5 (a) Impact of mass on STHT response on male objects (b) Impact of mass on DPMI response on male objects (c) Impact of mass on AM response on male objects (see online version for colours) (continued)

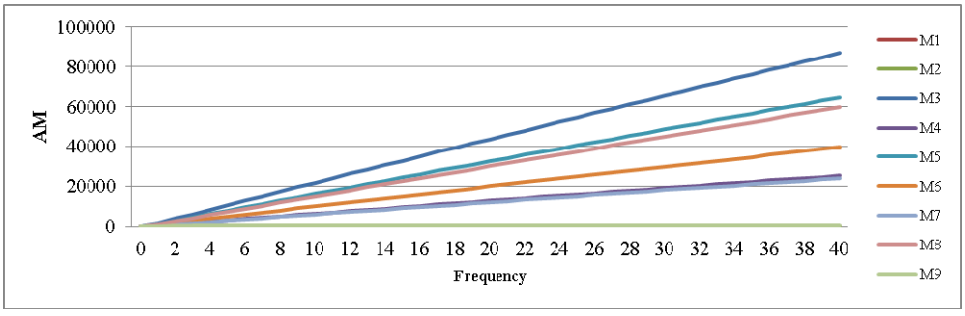

(c)

3.2 Analysis of impact of stiffness variation on the vibratory responses

Three different values of stiffness ($K4$), i.e., actual value, 50% increase and 50% decrease values are used to examine the effect of stiffness on the various biodynamic responses. The nature of impact is shown in Figure 6(a), 6(b) and (c), respectively. The analysis shows that by increasing the stiffness ($K4$), the biodynamic response (STHT) is increased in all three groups of male subjects.

Figure 6(a) shows that for young males (age between 18 years and 25 years), the response STHT is increasing with a decrease in the weight from the above curves. Hence, it can be stated that the STHT is inversely propositional to the weight of the body.

Figure 6(b) shows that for males (age between 25 years and 40 years), the response STHT is increasing with a decrease in weight, from the above curves. Hence, it can be stated that the STHT is inversely propositional to the weight of the body. But at a high frequency of more than 20 Hzs, STHT of average weight body decreases rapidly compared to high weight body.

Figure 6(c) observed that for males (age greater than 40 years), the response STHT is increasing with a decrease in the weight, from the above curves. Hence, it can be stated that the STHT is inversely propositional to the weight of the body.

Figure 6 (a) Impact of stiffness on STHT response on male (Group 1) objects (b) Impact of stiffness on STHT response on male (Group 2) objects (c) Impact of stiffness on STHT response on male (Group 3) objects (see online version for colours)

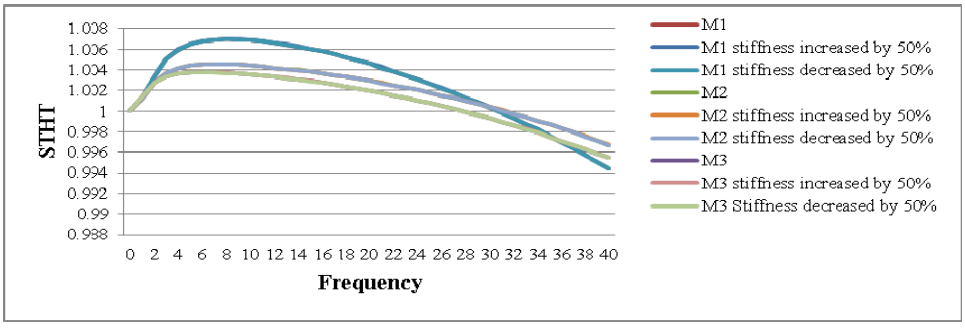

(a)

Figure 6 (a) Impact of stiffness on STHT response on male (Group 1) objects (b) Impact of stiffness on STHT response on male (Group 2) objects (c) Impact of stiffness on STHT response on male (Group 3) objects (see online version for colours) (continued)

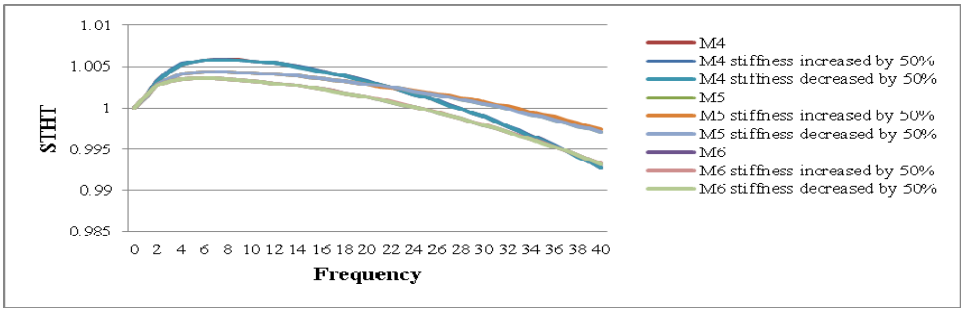

(b)

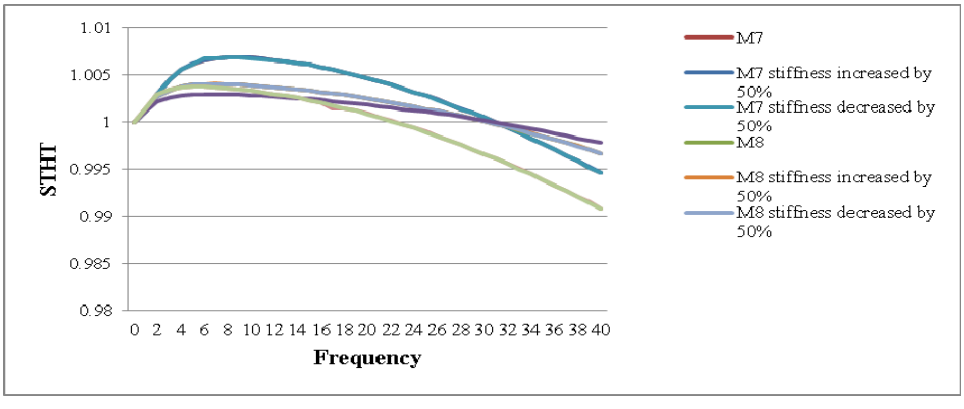

(c)

Figure 7(a) shows that for young males (age between 18 years and 25 years), the response DPMI increases with weight. Hence, it can be stated that the DPMI is directly propositional to the weight of the body.

From Figure 7(b), it is observed that for young male (age between years 25 and 40 years), the impact of the DPMI on the body with a higher weight (more than 80 kg) is low as compared to the body with an average weight (between 60 kg and 80 kg)

From Figure 7(c), it is observed that for young male (age more significant than 40 years), the impact of the DPMI on the body with a higher weight (more than 80 kg) is low as compared to the body with an average weight (between 60 kg and 80 kg)

Figure 7 (a) Impact of stiffness on DPMI response on male (Group 1) objects (b) Impact of stiffness on DPMI response on male (Group 2) objects (c) Impact of stiffness on DPMI response on male (Group 3) objects (see online version for colours)

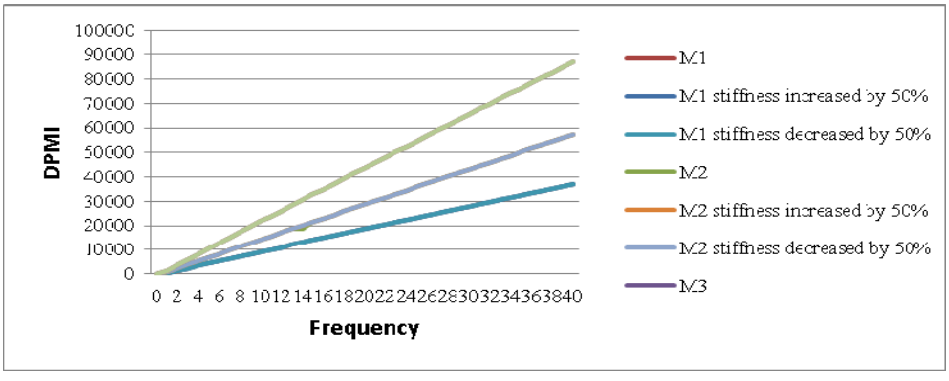

(a)

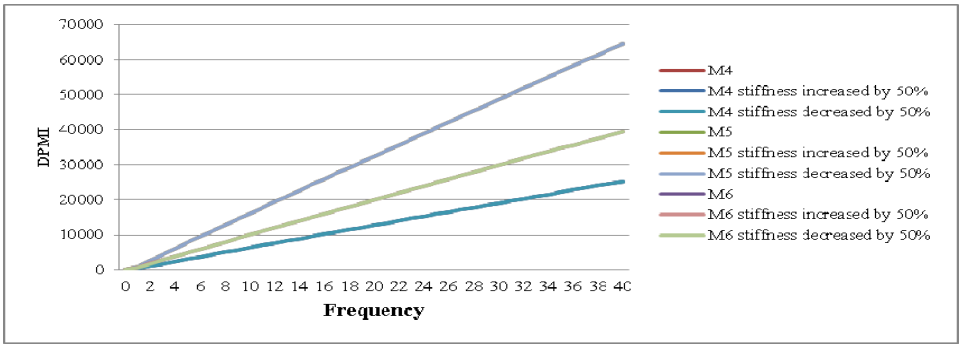

(b)

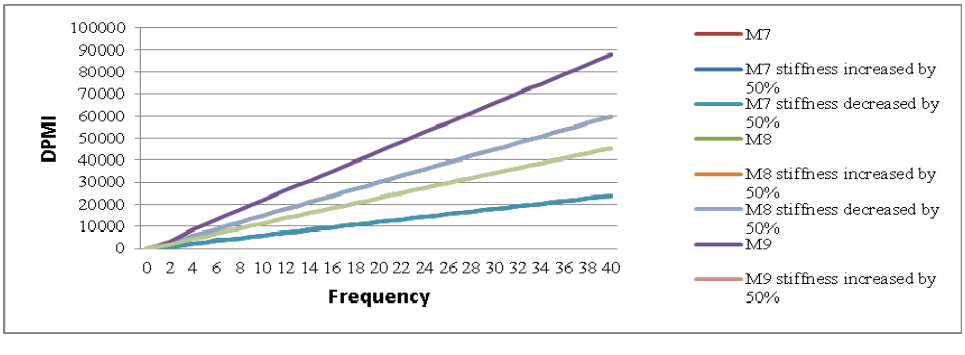

(c)

From Figure 8(a), it is observed that for young male (age between 18 years and 25 years), the impact of the AM on the body with a higher weight (more than 80 kg) is higher as compared to the body with an average weight (between 60 kg and 80 kg) and the body with lower weight (below 60 kg). From this, it can be concluded that the response AM is directly propositional to the body weight.

From Figure 8(b), it observed that for male (age between 25 years and 40 years), the impact of the AM on the body with a higher weight (more than 80 kg) is lower as compared to the body with average weight (between 60 kg and 80 kg) and the body with lower weight (below 60 kg).

Figure 8 (a) Impact of stiffness on AM response on male (Group 1) objects (b) Impact of stiffness on AM response on male (Group 2) objects (c) Impact of stiffness on AM response on male (Group3) objects (see online version for colours)

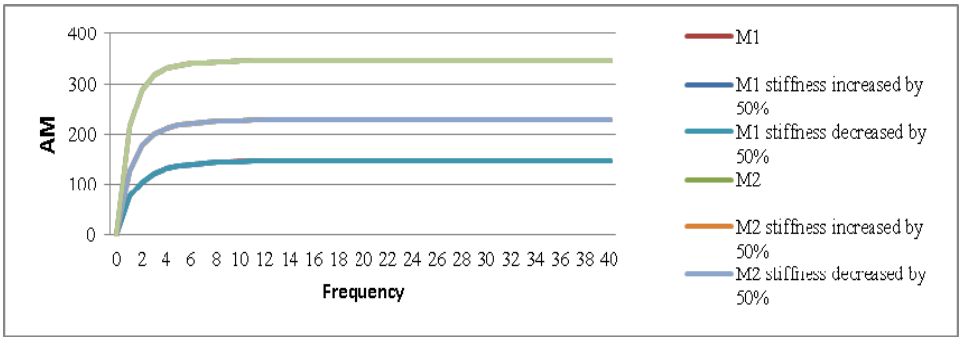

(a)

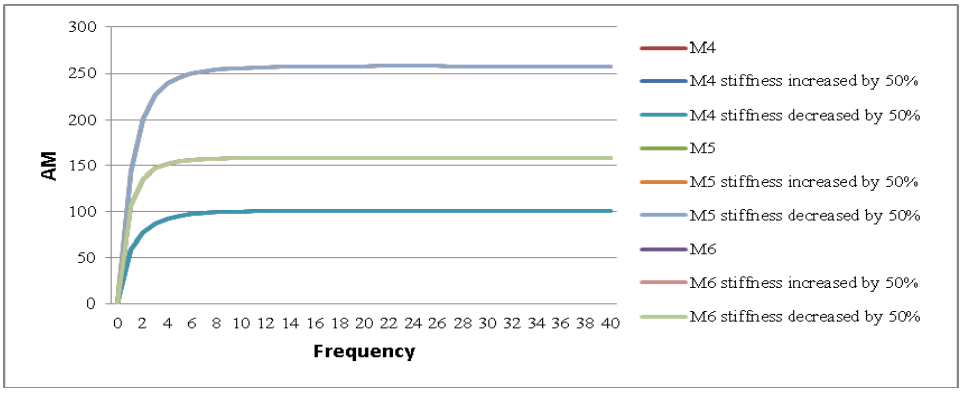

(b)

Figure 8 (a) Impact of stiffness on AM response on male (Group 1) objects (b) Impact of stiffness on AM response on male (Group 2) objects (c) Impact of stiffness on AM response on male (Group3) objects (see online version for colours) (continued)

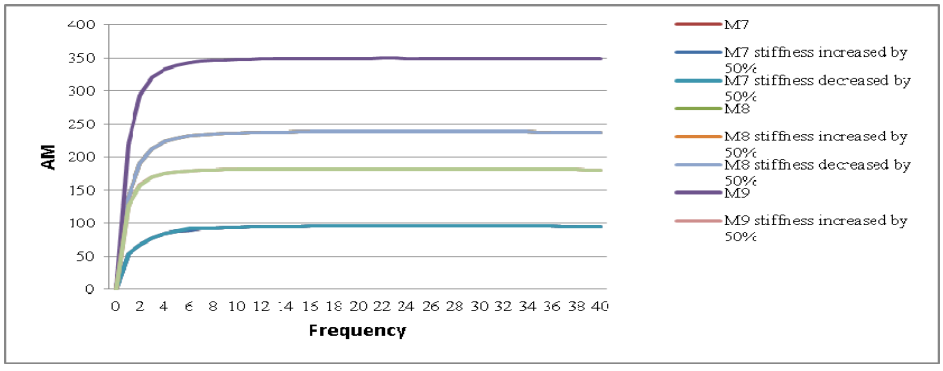

(c)

From Figure 8(c), it observed that for male (age greater than 40 years), the impact of the AM on the body with a higher weight (more than 80 kg) is higher as compared to the body with average weight (between 60 kg and 80 kg) and the body with lower weight (below 60 kg).

3.3 Analysis of impact of damping coefficient variation on the vibratory responses

From Figure 9(a), it observed that for young male (age between 18 years and 25 years), the impact of the STHT on the body with a higher weight (more than 80 kg) is lower as compared to the body with an average weight (between 60 kg and 80 kg) and the body with lower weight (below 60 kg). From this, it can be concluded that the response STHT is directly propositional to the body weight.

From Figure 9(b), it is observed that for male (age between 25 years and 40 years), the impact of the STHT on the body with a higher weight (more than 80 kg) is lower as compared to the body with an average weight (between 60 kg and 80 kg) and the body with lower weight (below 60 kg).

From Figure 9(c), it observed that for male (age more significant than 40 years), the impact of the STHT on the body with a higher weight (more than 80 kg) is lower as compared to the body with average weight (between 60 kg and 80 kg) and the body with lower weight (below 60 kg).

Figures 10(a), 10(b) and 10(c) observed that the impact of DPMI is severe in young male objects. The magnitude of the DPMI is directly propositional to the vibrational frequency. The curves are linear and increasing w.r.t. to the change in the frequency. From these figures, it is also cleared that the response DPMI increases with an increase in the magnitude of the damping coefficient and vice versa.

Figure 9 Impact of damping coefficient STHT response on male (Group 1) objects (b) Impact of damping coefficient STHT response on male (Group 2) objects (c) Impact of damping coefficient STHT response on male (Group 3) objects (see online version for colours)

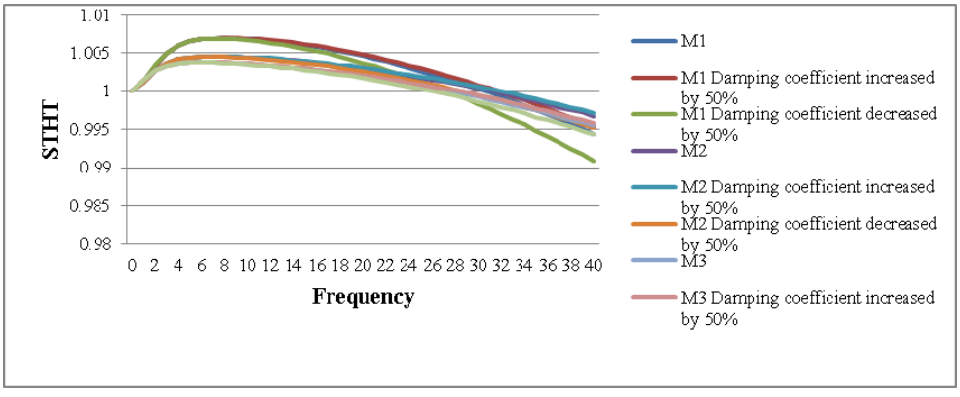

(a)

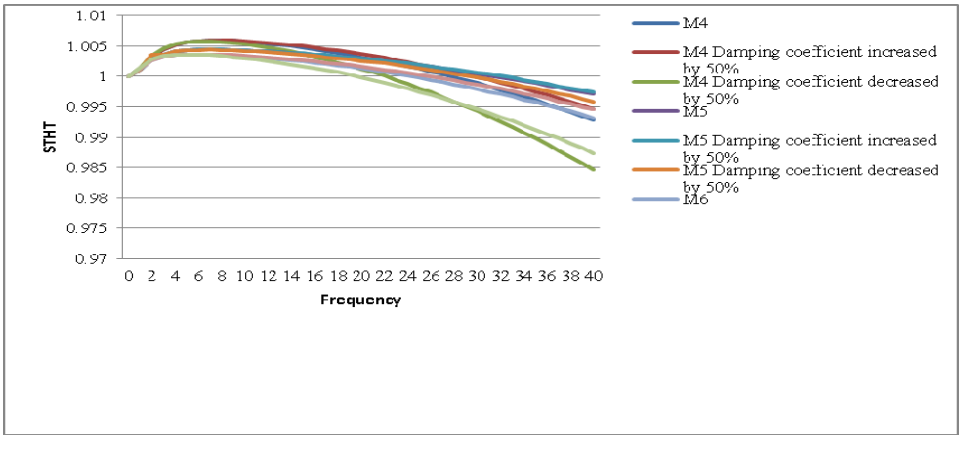

(b)

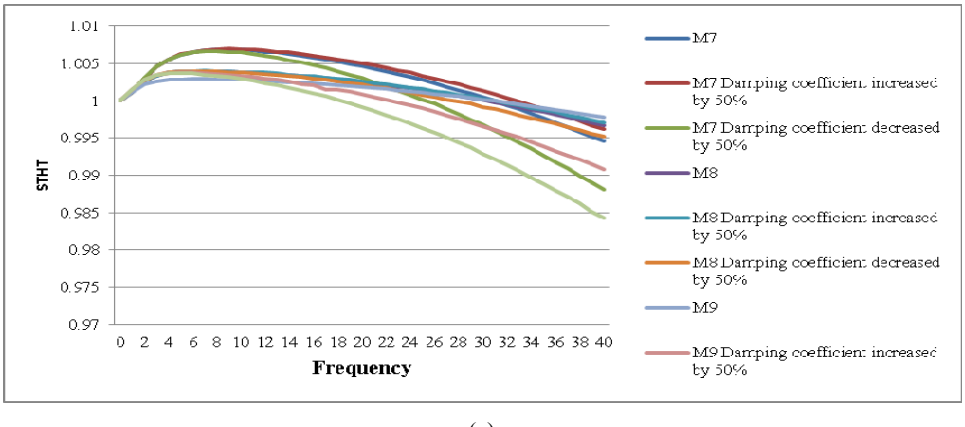

(c)

Figure 10 (a) Impact of damping coefficient DPMI response on male (Group 1) objects (b) Impact of damping coefficient DPMI response on male (Group 2) objects (c) Impact of damping coefficient DPMI response on male (Group 3) objects (see online version for colours)

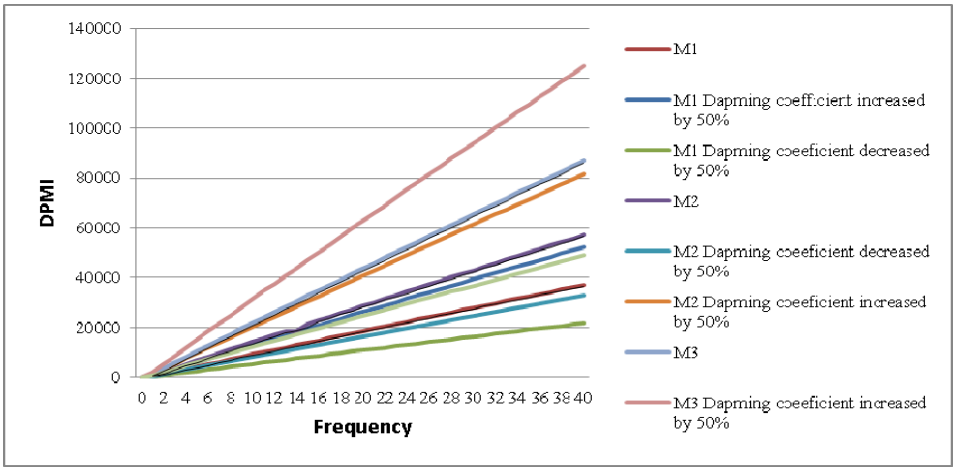

(a)

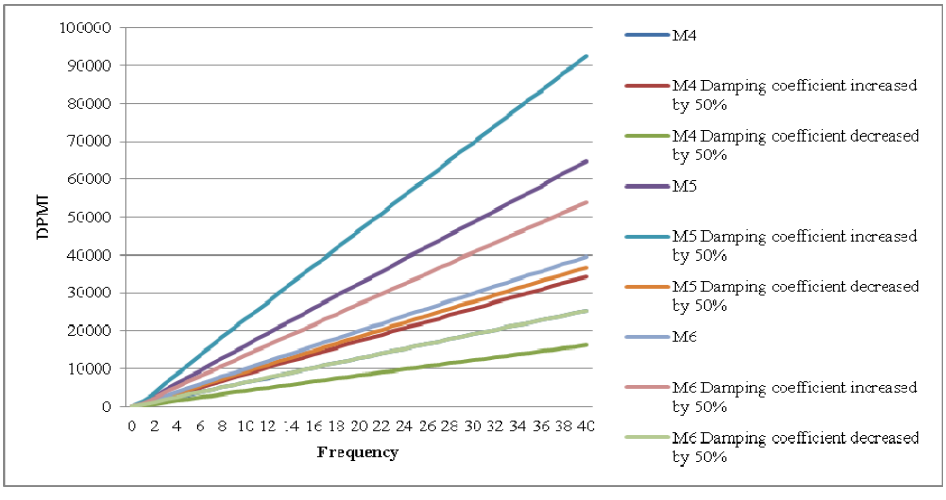

(b)

Figure 10 (a) Impact of damping coefficient DPMI response on male (Group 1) objects (b) Impact of damping coefficient DPMI response on male (Group 2) objects (c) Impact of damping coefficient DPMI response on male (Group 3) objects (see online version for colours) (continued)

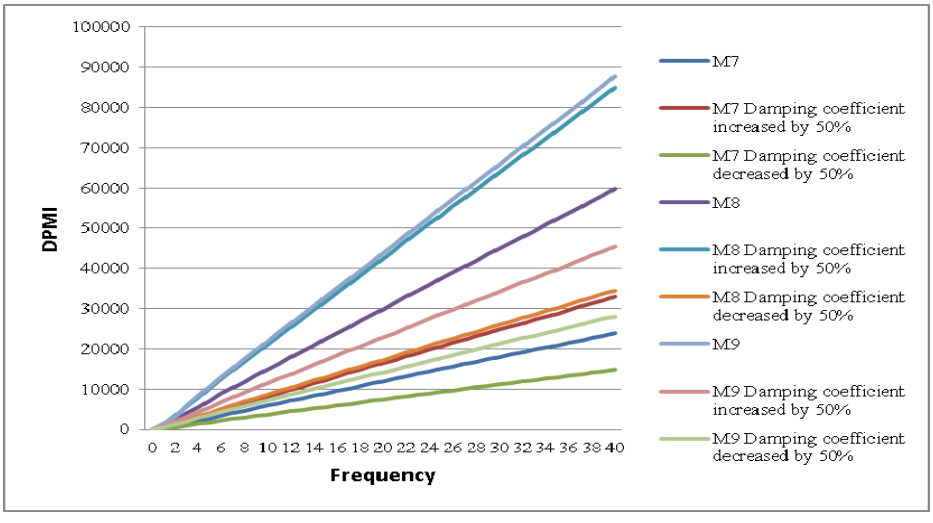

(c)

From Figure 11(a), 11(b) and 11(c), it is observed that the impact of AM is severe in the male objects whose age is more than 60 years and the weight is more than 80 kg as compared to the young male. Initially, the AM's magnitude is directly propositional to the vibrational frequency, and then it is constant. The curves are linear and increasing w.r.t. to the change in the frequency up to 6 Hz. From these figures, it is also cleared that the response AM increases with a decrease in the magnitude of the damping coefficient and via.

Figure 11 (a) Impact of damping coefficient AM response on male (Group 1) objects (b) Impact of damping coefficient AM response on male (Group 2) objects (c) Impact of damping coefficient AM response on male (Group 3) objects (see online version for colours)

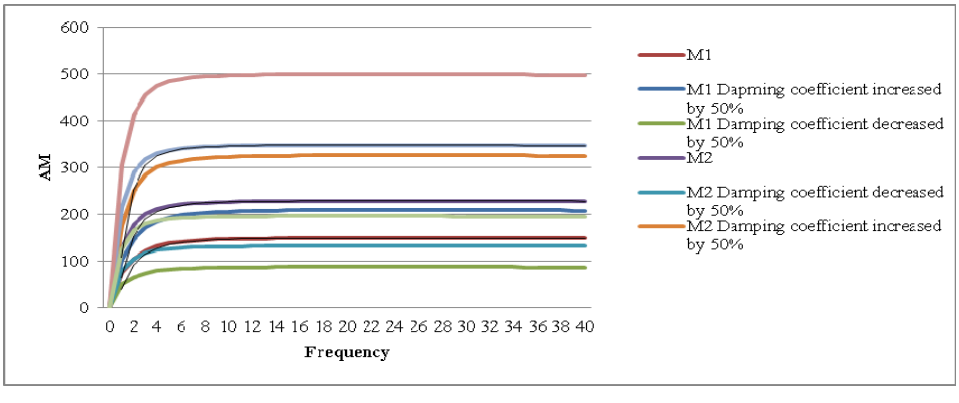

(a)

Figure 11 (a) Impact of damping coefficient AM response on male (Group 1) objects (b) Impact of damping coefficient AM response on male (Group 2) objects (c) Impact of damping coefficient AM response on male (Group 3) objects (see online version for colours) (continued)

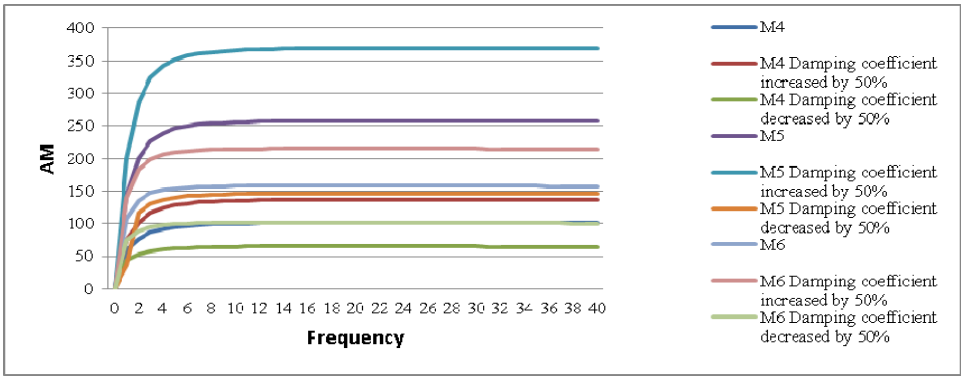

(b)

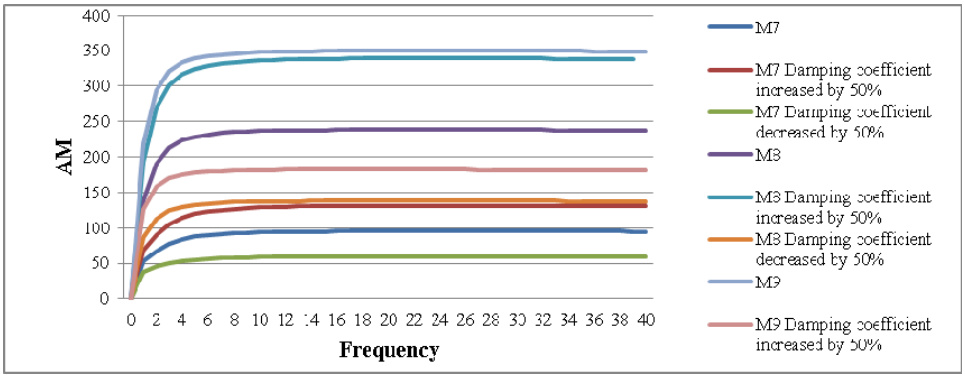

(c)

4 Conclusions

The automobile is an essential part of our life. The literature related to injuries and the discomfort due to the long and continuous traveling shows the need for comfortable automobile seats that minimise injuries during the traveling. To highlight the nature of injuries and their severity in various age groups, male subjects and low and heavyweight male objects have been examined and presented in this work. The drivers of heavy-duty vehicles like tractors and trucks expose a high level of vibration in their occupational lives, which causes vibration-induced injuries or disorders. This study aims to evaluate the response of seated posture spring-mass-damper system human body model exposure to Whole-BodyVibration. The seated human four Degree of Freedom (DOF) biodynamic model analysed. The body parameters related to the model are calculated based on body features and some biodynamics standards. The response is calculated and tabulated in the table. The impact of various parameters such as age, weight, and gender were examined

by changing the different body-related parameters. For the analysis purpose, MINITAB 18 software was used effectively.

The presented work is instrumental in automobile industries to design the automobile seats as per the outcomes and minimise the impact of vibrations on the seated human body. The development of the presented work will help the passenger and drivers take preventive measures to avoid injuries and permanent severe damage.

Acknowledgements

The authors would like to thank everyone, just everyone!

References

Abdeen, M.A.M. and Abbas, W. (2010) 'Analytic investigation and numeric prediction for biodynamic response of the seated human body', *Journal of American Science*, pp.228–239.

Bai, X.X., Xu, S.X., Cheng, W. and Qian, L-J. (2017) 'On 4-degree of freedom biodynamic models of seated occupants: lumped parameter modelling', *Journal of Sound and Vibration*, Vol. 204, pp.122–141.

Fairley, T.E. and Griffin, M.J. (1989) 'The apparent mass of the seated human body: vertical vibration', *Journal of Biomechanics*, Vol. 22, No 2, pp.81–94.

Feng, K. (2019) 'Adaptive automobile seat design based on ergonomic principle', *International Journal of Vehicle Structures and Systems*, Vol. 11, No. 5, pp.589–594.

Govindan, R. and Harsha, S.P. (2018) 'Effect of low-frequency vibration on human body in standing position exposed to railway vehicle', *International Journal of Vehicle Structures and Systems*, Vol. 10, No. 3, pp.160–164.

Gupta, T.C. (2007) 'Identification and experimental validation of damping ratios of different human body segments through anthropometric vibratory model in standing posture', *Journal of Biomechanical Engineering*, Vol. 129, No. 4, pp.566–574.

Liang, C-C. and Chiang, C-F. (2006) 'A study on biodynamic models of seated human subjects exposed to vertical vibration', *International Journal of Industrial Ergonomics*, Vol. 36, pp.869–890.

Liu, C., Qiu, Y. and Griffin, M.J. (2017) 'Dynamic forces over the interface between a seated human body and a rigid seat during vertical whole body vibration', *Journal of Biodynamics*, Vol. 61, pp.176–182.

Marzbanrad, J., Rad, Y.A. and Afkar, A. (2010) 'Vibration isolation of a Ga optimized biomechanical model of a railway passenger using magneto rheological damper seat suspension', *International Journal of Vehicle Structures and Systems*, Vol. 2, No. 1, pp.1–8.

Neil, J. (2005) 'Mansfield, impedance methods (apparent masses, driving point mechanical impedance and absorbed power) for the assessment of the biomechanical response of the seated human to whole body vibration', *Industrial Health*, Vol. 43, pp.378–389.

Nigam, S.P. and Malik, M. (1987) 'A study on a vibratory model of a human body', *Journal of Biomechanical Engineering*, Vol. 109, No. 2, pp.148–153.

Phate, M.R. and Gaikwad, P. (2018) 'Exploring biodynamic response (apparent masses) of a seated human body exposed to external excitation in vertical direction', *International Journal of Industrial Engineering and Production Research*, Vol. 29, No. 4, pp.415–428.

Phate, M.R. and Sahu, D. (2020) 'Simulink based biodynamic model for the human arm Subjected to vibration', *Industrial Engineering Journal*, Vol. 13, No. 3, pp.1–13.

Phate, M.R., Gaikwad, P. and Toney, S. (2022) 'Analysis of seat to head transmissibility of the seated human body using artificial neural network', *Institution of Engineers Series C*, pp.1–15.

Phate, M.R., Toney, S.B. and Phate, V.R. (2019) 'Prediction and analysis of apparent masses (AM) of anthropometric based human seated posture', *Industrial Engineering Journal*, Vol. 12, No. 11, pp.1–14.

Rao, M.J., Sivaprakasam, S.P. and Arora, G.Y. (2018) 'Ride comfort of urban minibus driver through optimization of seating parameters and vehicle speed', *International Journal of Vehicle Structures and Systems*, Vol. 10, No. 6, pp.411–414.

Sastry, D.A.V.R., Ramana, K.V., Rao, N.M., Kumar, M.P. and Reddy, V.S.S.R.C. (2018) 'Evaluation of human exposure to vibrations using quarter car model with semi-active suspension', *International Journal of Vehicle Structures and Systems*, Vol. 10, No. 4, pp.268–272.

Wang, W., Rakhejaa, S. and Boileau, P.E. (2008) 'Relationship between measured apparent mass and seat-to-head transmissibility responses of seated occupants exposed to vertical vibration', *Journal of Sound and Vibration*, Vol. 314, pp.907–922.